ISSN 2007-9737

Ultrasound Synthesized Carbon Nanoparticles and Their Photoluminescence Property

Enrique Esparza-Alegría[1], Ismael A. Garduño-Wilches[2],
Rocío Guadalupe Casañas-Pimentel[1], Hector Báez Medina[3],
Eduardo San Martín Martínez[1,*]

[1] Instituto Politécnico Nacional,
Centro de Investigación en Ciencia Aplicada y Tecnología Avanzada,
Ciudad de Mexico,
Mexico

[2] Cátedras Conacyt Instituto Politécnico Nacional,
Centro de Investigación en Ciencia Aplicada y Tecnología Avanzada,
Ciudad de Mexico,
Mexico.

[3] Instituto Politécnico Nacional,
Centro de Investigación en Computación,
Ciudad de Mexico,
Mexico

esanmartin@ipn.mx

Abstract. Whenever nanomaterials are used to address health science-related problems, the qualities of biocompatibility and biodegradability must be kept in mind, since they ensure that the materials circulating through the carrier biological system used to diagnose or treat a disease are properly eliminated once their function is fulfilled, interfering as little as possible with the normal functioning of the carrier. For this reason, carbon and synthesizing carbon nanostructures (CNPs) were selected to develop diagnostic probes in tumor tissues. Glucose (1 M sol. in deionized water) was taken as a carbon precursor, and hydrolysis was performed in an acidic (36% HCl) and basic (1 M NaOH) medium, using ultrasound for 4 h continuous, at 25 kHz, 30 °C, and a power of 90%. The sonicated solutions are neutralized at pH 7 and centrifuged to separate the supernatant, where the carbon nanostructures are obtained. The NPsC were characterized by UV-Vis spectrometry, and the photoluminescent properties by spectrofluorometer and IVIS Lumina, transmission electron microscopy (TEM), and FTIR. The results obtained were that the NPsC have a high emission wavelength (650 nm) when excited at 450 nm, for the NPsC in a basic medium maintain a higher intensity than the NPsC synthesized in an acidic medium.

Keywords. Carbon; ultrasound; glucose; UV-Vis; spectrofluorometer; IVIS lumina.

1. Introduction

In recent years, it has been discovered that photons originate from various processes such as The Bremsstrahlung effect where photons are produced by the deceleration of electric charges [1], the collision and annihilation between particles and antiparticles [2], Cherenkov radiation [3], chemical reactions (chemiluminescence) [4], chemical reactions in living beings (bioluminescence) [5], the breaking of bonds in materials when they are scratched, rubbed

doi: 10.13053/CyS-30-1-6345

or pulverized (triboluminescence) [6], the production of photons by non-destructive pressure action in certain solids (piezoluminescence) [7], by a combination of photonic and piezoelectric effects [8].

One way to encompass a large majority of phenomena that produce photons is luminescence, defined as the emission of energy in the form of electromagnetic radiation resulting from a non-necessarily thermal excitation of electrons in atoms, molecules, polymers, and crystals. When excited electrons undergo a transition to a lower energy state, photon emission occurs [9-12].

When atoms come together to form molecules, the electron densities corresponding to the outer orbitals of the valence electrons tend to combine so that the electrons now occupy more space than before, and the resulting system is energetically smaller and more stable when compared to the states of the constituent atoms separately. Thus, the electrons occupy these new configurations and molecular orbitals belonging to the molecule as a whole and can still undergo energy transitions just as they would in isolated atoms.

In a solid, the small group or fraction of atoms, ions, molecules, or crystals that exhibit luminescence are known as luminescence centers and are usually point defects in the solid's lattice. The ground state of a luminescence center is defined as that place where the lowest energy is, and therefore the system (atom, ion, molecule, or crystal) tends to remain there most of the time.

It is well known that not all materials show luminescence, and the reason is that photon emission processes compete with the so-called non-emissive (or non-radiative) returns to the ground state in which the energy of the excited state is used to vibrate the crystal lattice of the material or to heat it.

Among all the ways of promoting electrons to excited states, the work of the present research will focus on those materials that produce the phenomenon of luminescence from the absorption of electromagnetic radiation (i.e., other photons), which is known as photoluminescence.

Materials that exhibit this phenomenon have found application in fields such as aerodynamics, marine imaging, fluid dynamics, and marine microbiology [1].

Currently, the most promising field where the phenomenon of photoluminescence has found a place in medical imaging [2], which is a field that encompasses the set of techniques and procedures that allow obtaining images of the human body or parts of it for clinical purposes (mainly to diagnose or examine diseases) or for research for medical-biological sciences (including the study of anatomy and its functions).

Fundamentally, among the imaging techniques are radiodiagnosis, nuclear medicine, and radiotherapy.

Among the different techniques that exist for the synthesis of photoluminescent materials, the method of hydrolysis assisted by ultrasonic agitation [3] is widely used and today continues to be the subject of study due to its simplicity and the wide range of variables available for the study and synthesis of photoluminescent materials.

In a typical synthesis, the precursor is placed in an acidic (or basic) solution inside a glass container that is introduced into a vat of water whose walls produce a mechanical movement that generates vibrations at frequencies above the audible range (more than 20 kHz). This generates mechanical waves propagating in the liquids that produce

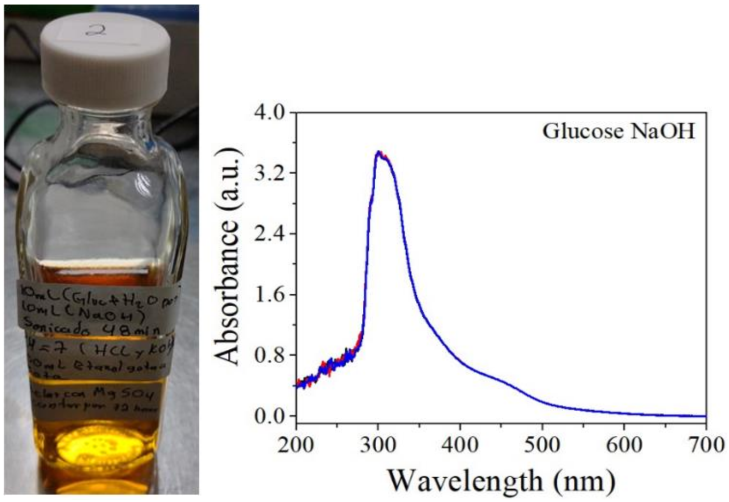

Fig. 1. Carbon NPs sample synthesized by ultrasound-assisted basic hydrolysis (NaOH) of 1 molar glucose solution

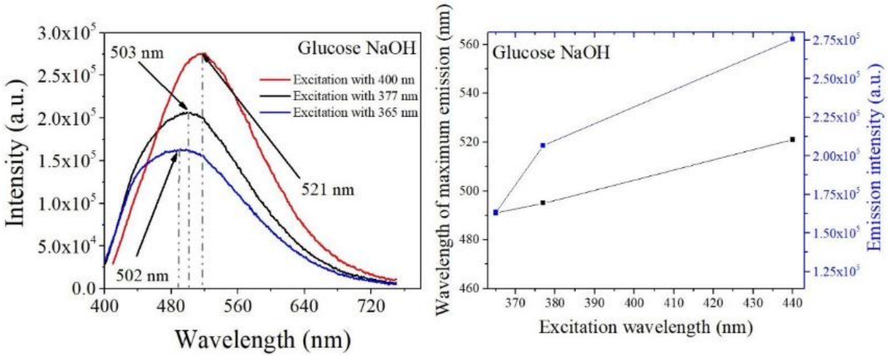

Fig. 2. On the left, emission spectra of carbon NPs synthesized by ultrasound-assisted basic hydrolysis (NaOH) of a 1 molar glucose solution. On the right are plots of maximum emission wavelength and emission intensity versus excitation wavelength for the same sample

zones of high and low pressure. In the low-pressure zones, small vacuum bubbles are created where the surrounding liquid evaporates and fills with water vapor.

The vapor bubbles migrate to high-pressure zones where they collapse adiabatically and violently on themselves.

This implosion is accompanied by the release of energy, thus reaching high pressures and temperatures that are used for hydrolysis [4, 5]. It has been reported that, both in the implosion of the bubble and at the boundary between the liquid and its vapor, OH- and H+ ions are produced, which are also used in the hydrolysis process [4-6].

Among the various existing nanostructures, carbon NPs are the most used for applications in biological and health sciences because they have two main advantages: The first is that they can be synthesized from low-cost and

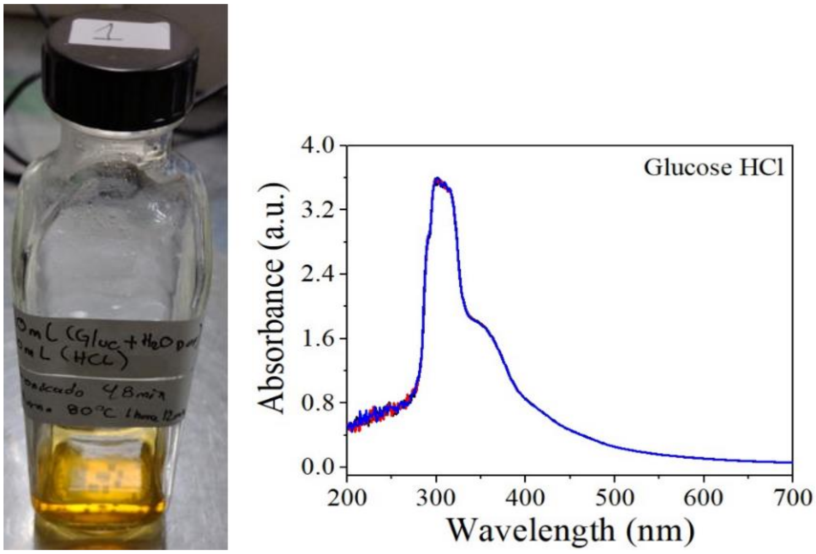

Fig. 3. Carbon NPs sample synthesized by ultrasound-assisted acid hydrolysis (HCl) of 1 molar glucose solution.

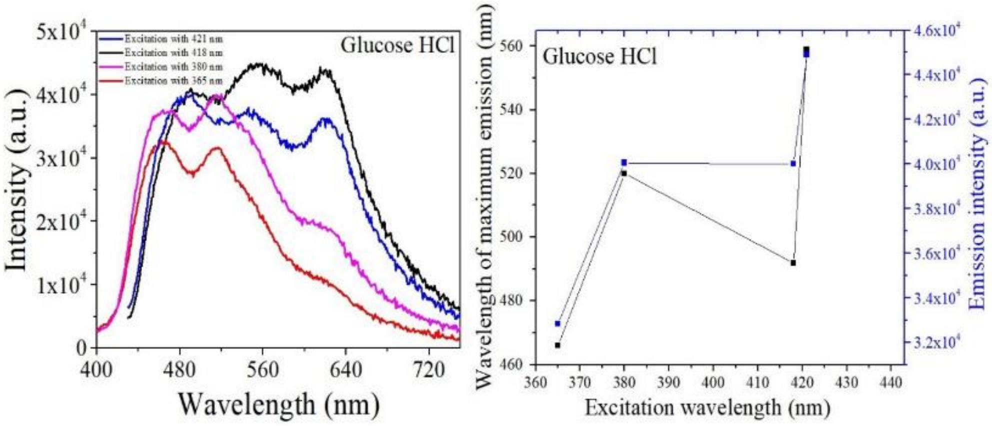

Fig. 4. On the left, emission spectra of carbon NPs synthesized by ultrasound-assisted acid hydrolysis (HCl) of 1 molar glucose solution at 72 min, 80°C. On the right are plots of maximum emission wavelength and emission intensity versus excitation wavelength for the same sample.

highly available natural organic precursors such as chitosan, lysine, dextrin, citric acid, etc.

The second advantage is that once synthesized, carbon NPs themselves are environmentally friendly and have high biocompatibility and biodegradability in living beings.

So, in the present work, carbon nanostructures (NPsC) will be synthesized by ultrasound-assisted hydrolysis.

2. Materials and Methods

For the synthesis of carbon NPs by this method, 3 solutions are prepared: A solution of 100 ml of Glucose precursor ($C_6H_{12}O_6$) (Sigma-Aldrich, Lot. 212K08902) in deionized water (with a Barnstead EASY PURE deionizer at a resistivity of 18.2 MΩcm) at 1 M, which will be named Sol (Prec). A solution of 50 ml of NaOH (Meyer) in deionized water at 1 M, will be named Sol (NaOH), and finally 50 ml of 36~38% HCl (Meyer), which will be identified as Sol (HCl).

With the three previous solutions, the following two solutions are now prepared: 50 ml of Sol (Gluc) is combined with 50 ml of Sol (NaOH). This solution is known as Sol(A), and 50ml of Sol (Gluc) is combined with 50ml of Sol (HCl). This solution is known as Sol(B).

The Sol(A) and Sol(B) solutions are then sonicated separately for 4 continuous hours in an ultrasonic bath (Elma model TI-H-5, Germany). At 25 kHz, 30 °C temperature, and 90% power.

After sonication, the pH of the 100 ml of Sol(A) is adjusted to 7 with HCl or NaOH solutions in deionized water. Only 20 ml of this solution is taken, and 100 ml of ethanol (Meyer) is added drop by drop under stirring.

To the resulting solution, 12% by weight of MgSO4 (Mallinckrodt Pharmaceuticals) is added, stirred for 20 minutes, and the resulting solution is left to stand for 24 h to remove the dissolved salts.

The solutions are subjected to centrifugation at 6,000 x g for 15 minutes (Eppendorf Centrifuge 5430R). The carbon NPs dissolved in the supernatant of the solution are recovered for characterization.

In case of the 100 ml of Sol(B), were also neutralized to pH 7 and then heated to 80°C for 6 hours in a convection oven (Felisa, Mexico). After cooling to room temperature, the solution is centrifuged at 3,800 x g for 15 minutes, and once this process is finished, the supernatant containing the carbon NPs is recovered.

2.1. Characterization by UV-Vis Spectroscopy

NPsC were characterized with a UV-Vis spectrophotometer (Genesis 10S UV-Vis from Thermo Scientific). Two mL of the supernatant was placed in a quartz cuvette, and absorbance spectra were obtained with wavelengths between 250 nm and 700 nm.

2.2. Characterization by Photoluminescence Spectroscopy

The characterization method was carried out with a spectrofluorometer (Edinburgh Instruments model FS5, United Kingdom). 2 mL of the sample supernatant was placed in a quartz cuvette and irradiated at different excitation wavelengths. As a result of the interaction between photons and NPsC, emission spectra were obtained.

The other evaluation of the photoluminescent properties was carried out with an IVIS imaging device (IVIS Lumina XRMS Series III Perkin Elmer, USA), 300 µL of the sample supernatant was placed in opaque polystyrene 96-well microplates for analysis and irradiated at different excitation wavelengths. As a result, emission spectra were obtained.

2.3. Characterization by Transmission Electron Microscopy (TEM)

Approximately 2 µL of the supernatant was deposited on carbon-coated 200-mesh copper grids (Electron Microscopy Science, USA) and allowed to dry at room temperature. The microstructure and size of the NPsC on the copper grids were evaluated by TEM

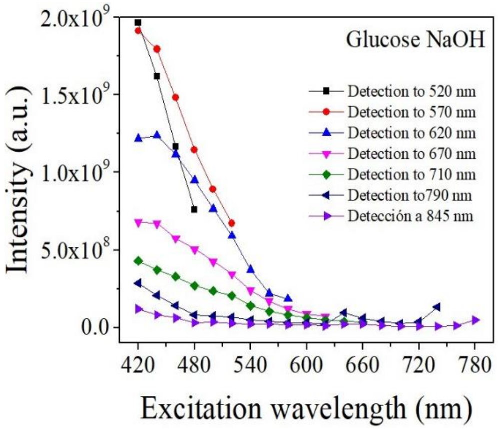

Fig. 5. Photoluminescence spectra obtained with the IVIS Lumina of the sample synthesized from glucose and NaOH, after 1h of sonication.

(Transmission Electron Microscope TEM JEM-ARM 200F JEOL, Japan).

2.4. Characterization by Fourier Transform Infrared Spectroscopy (FTIR)

20 µL of the supernatant was deposited on the diamond sensor of an FTIR Spectrometer Cary 630, and FTIR spectra were obtained.

3. Results and Discussion

3.1. Photoluminescence

By performing the synthesis of carbon NPs by basic hydrolysis (NaOH) of a 1 molar glucose solution assisted by ultrasound, the solution of the left image of Figure 1 was obtained, to which UV-Vis spectroscopy studies were applied, the graph on the right of the same figure. The absorbance spectra show a band around 230-300 nm. The absorbance maximum between 230 and 320 nm for carbon NPs is associated with π-π* type transitions of C-C bonds, while the maxima around 330 nm are attributed to n-π* type transitions attributed to C-O type bonds [7-9].

The sample was also characterized by photoluminescence spectroscopy, obtaining the emission spectra in the left image of Figure 2, and from them, the graphs on the right were constructed, of maximum emission wavelength and emission intensity against excitation wavelength.

Increasing the excitation wavelengths of 365, 377, and 400 cm-1 in the NPsC produces a shift in the emission wavelengths to higher values, reaching 502, 503, and 521 cm-1, also favoring increases in the emission intensity, obtaining values close to 280,000 (u.a.).

On the other hand, the results of the synthesis of carbon NPs by acid hydrolysis (HCl) of 1 molar glucose solution assisted by ultrasound, obtained the solution in the left image of Figure 3, to which UV-Vis spectroscopy studies were applied, right image of the same figure.

As for carbon NPs synthesized with NaOH, the absorbance maximum between 230 and 320 nm is associated with π-π* transitions of C=C bonds, while the maximum around 330 nm is associated with n-π* transitions of C=O bonds [7-9].

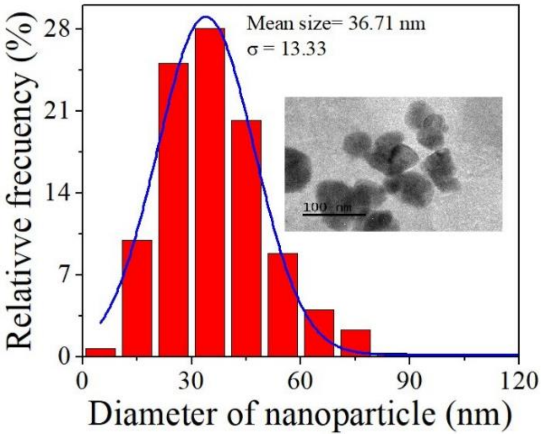

Fig. 6. Histogram of NPsC synthesized from Glucose and NaOH. The histogram shows an average diameter of 36.71 nm and a σ of 13.33.

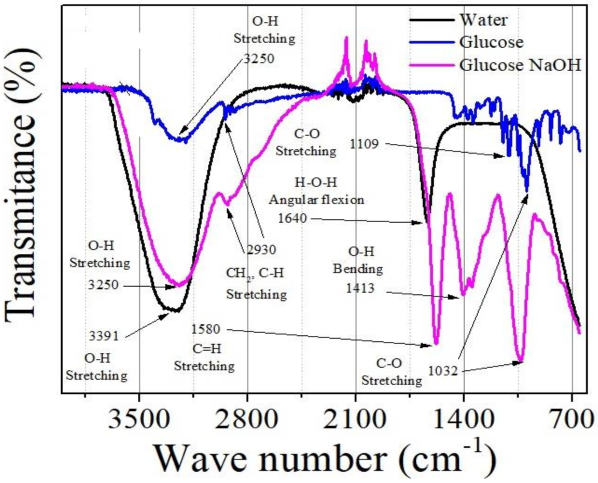

Fig. 7. FTIR spectrum of NPsC synthesized from glucose and NaOH. Some interactions, such as O-H stretching, C-C stretching, and C-C bending, can be observed.

The sample synthesized in an acidic environment was also characterized by photoluminescence spectroscopy, obtaining the emission spectra of the left image of Figure 4, and from them, the graphs on the right of maximum emission wavelength and emission intensity against excitation wavelength. The results of photoluminescence spectroscopy for the acid synthesis (HCl) show higher emission wavelength values than those obtained with NaOH. If we make the comparison with 400 nm excitation for the sample synthesized with NaOH, 521 nm of emission is obtained now for the synthesis in HCl, excited at 421 nm, and the emission wavelength is 560 nm. These small differences in the emission wavelengths could improve the diagnosis of cancer cells, which would avoid shielding by other compounds in the blood fluid. However, the maximum luminescence intensity of NPsC in acid (45,000 u.a.) is lower than that obtained in a basic medium (275,000 u.a.).

3.2. Photoluminescence by IVIS Lumina

When performing photoluminescence spectroscopy studies at IVIS Lumina, the graph in Figure 5 was obtained. It shows that carbon NPs present absorption and emission beyond wavelengths of 600 nm. When the CNPs are excited at 450 nm, the intensity is 2.00 x 109, with an emission wavelength of 570 nm. If the excitation wavelength is increased, the emission intensity decreases.

When the emission wavelength is increased to values greater than 670 nm, the intensity decreases, similarly to longer excitation wavelengths. These results indicate that NPsC, due to their size and geometry, have a band gap, which allows them to be excited at a maximum of 450 nm and emit at 650 nm with the highest intensity.

3.3. Transmission Electron Microscopy (TEM)

From the TEM studies, the following histogram was obtained, which shows an average diameter of 36.71 nm for NPsC synthesized from glucose and NaOH.

The size of NPsC of 36 nm or less confirms the luminescent properties because they are composed of a carbon core with different crystalline domains and whose electrons of the atoms are distributed in different orbital hybridizations [22] and impurities that form the so-called electron energy traps that, according to the literature [23], are mainly responsible for the electronic transitions that cause photoluminescence.

3.4. Fourier Transform Infrared Spectroscopy

The graphs in Figure 7 show FTIR spectra of water, glucose, and NPsC synthesized in NaOH. FTIR spectra were performed for each component to observe the participation of functional groups in the formation of NPsC.

The water spectrum has a bond stretching vibration at 3250 cm-1 characteristics of the -OH group, and another bending vibration at 1640 cm-1 corresponding to H-O-H. Glucose presents functional group vibrations of the O-H, C-H, C-O, and C-C types, both stretching and bending.

When glucose molecules are hydrolyzed in basic and acidic media, the C-C and C-O-C bonds are broken, and in the hydrolysis, H2O is generated, as well as C-OH, C-C, and C-O molecules that are identified by their vibration in the FTIR spectrum.

4. Conclusions

From ultrasound-assisted hydrolysis of glucose, carbon nanostructures with diameters of around 36.71 nm were obtained, which exhibit the phenomenon of photoluminescence when excited at the absorption wavelength of 450 nm and emitting at wavelengths greater than 650 nm.

The highest intensity of luminescence emission is observed when NPsC are synthesized in a basic medium (275,000 u.a.), and in acid, it is lower (45,000 u.a.).

UV-Vis spectroscopy studies show the presence of π-π* type transitions of C=C bonds and n-π* of C=O. FTIR studies indicate that functional groups such as O-H, C-H, C-O, and C-C are present in NPsC and the presence of water as a consequence of glucose hydrolysis.

References

1. **Haug, E., Nakel, W. (2004).** The Elementary Process of Bremsstrahlung. World Scientific.
2. **Berestetskii, V.B., Lifshitz, E.M., Pitaevskii, L.P. (1982).** Quantum Electrodynamics. Volume 4, Butterworth-Heinemann.
3. **Bolotovskii, B.M. (2009).** Vavilov–Cherenkov Radiation: Its Discovery and Application, Physics-Uspekhi, Vol. 52, pp. 1099.
4. **Mao, D., Wu, W., Ji, S. (2017).** Chemiluminescence-Guided Cancer Therapy Using a Chemiexcited Photosensitizer. Chem, Vol. 3, pp. 991–1007.
5. **Brodl, E., Winkler, A., Macheroux, P. (2018).** Molecular Mechanisms of Bacterial Bioluminescence. Computational And Structural Biotechnology Journal, Vol. 16, pp. 551–564.
6. **Freund, F.T. (2016).** Nature of the Electronic Charge Carriers Involved in Triboluminescence. Triboluminescence, pp. 17–37.
7. **Gan, J., Kang, M.G., Meeker, M.A. (2017).** Enhanced Piezoluminescence In Non-Stoichiometric ZnS: Cu Microparticle Based Light Emitting Elastomers. Journal Of Materials Chemistry C, Vol. 5, pp. 5387–5394.
8. **Hao, J., Xu, C.N. (2018).** Piezophotonics: From Fundamentals and Materials to Applications. MRS Bulletin, Vol. 43, pp. 965–969.
9. **Gribkovskii, V. (1998).** Theory of Luminescence. Luminescence of Solids, pp. 1–43.
10. **Garlick, G. (1958).** Luminescence, Light and Matter, II Licht Und Materie II, pp. 1–128.
11. **Murthy, K., Virk, H.S. (2014).** Luminescence Phenomena: An Introduction. Defect and Diffusion Forum, pp. 1–34.
12. **Ronda, C.R. (2007).** Luminescence: From Theory to Applications. John Wiley & Sons.
13. **Schäferling, M. (2012).** The Art of Fluorescence Imaging with Chemical Sensors, Angewandte Chemie International Edition, Vol. 51, pp. 3532–3554.
14. **Liu, J., Lécuyer, T., Seguin, J. (2019).** Imaging and Therapeutic Applications of Persistent Luminescence Nanomaterials, Advanced Drug Delivery Reviews, Vol. 138, pp. 193–210.
15. **Li, H., He, X., Liu, Y. (2011).** One-Step Ultrasonic Synthesis of Water-Soluble Carbon Nanoparticles with Excellent Photoluminescent Properties. Carbon, Vol. 49, pp. 605–609.
16. **Hua, I., Hoechemer, R.H., Hoffmann, M.R. (1995).** Sonolytic Hydrolysis of P-Nitrophenyl Acetate: The Role of Supercritical Water, The Journal Of Physical Chemistry, Vol. 99, pp. 2335–2342.
17. **Baranchikov, A.Y., Ivanov, V.K., Tretyakov, Y.D. (2007).** Sonochemical Synthesis Of Inorganic Materials. Russian Chemical Reviews, Vol. 76, pp. 133.
18. **Yim, B., Nagata, Y., Maeda, Y. (2002).** Sonolytic Degradation Of Phthalic Acid Esters In Aqueous Solutions Acceleration of Hydrolysis by Sonochemical Action. The Journal of Physical Chemistry A, Vol. 106, pp. 104–107.
19. **Gao, P., Xie, Z., Zheng, M. (2022).** Small Nanoparticles Bring Big Prospect: The Synthesis Modification Photoluminescence And Sensing Applications of Carbon Dots, Chinese Chemical Letters, Vol. 33, pp. 1659–1672.
20. **Sendão, R.M., Crista, D.M., Afonso, A.C.P. (2019).** Insight into The Hybrid Luminescence Showed By Carbon Dots And Molecular Fluorophores In Solution, Physical Chemistry Chemical Physics, Vol. 21, pp. 20919–20926.
21. **Zhu, S., Song, Y., Zhao, X. (2015).** The Photoluminescence Mechanism in Carbon Dots Graphene Quantum Dots Carbon Nanodots and Polymer Dots Current State And Future Perspective. Nano Research, Vol. 8, pp. 355–381.
22. **Kaczmarek, A., Hoffman, J., Morgiel, J. (2021).** Luminescent Carbon Dots Synthesized By the Laser Ablation of Graphite

In Polyethylenimine And Ethylenediamine, Materials, Vol. 14, pp. 729.

23. **Sun, Y.P., Zhou, B., Lin, Y. (2006).** Quantum-Sized Carbon Dots for Bright and Colorful Photoluminescence, Journal of the American Chemical Society, Vol. 128, pp. 7756–7757.

Article received on 15/07/2025; accepted on 09/02/2026.
**Corresponding author is Eduardo San Martín Martínez.*